

atoms in a molecule or among all nearest neighbors. Further iterations could be added.

Options other than eqs 12 and 13 could also be considered for combining electrostatic and covalent forces. Some authors<sup>8,10</sup> have proposed that covalent bonding weakens as charge separation occurs. Van der Waals interactions between nonbonded atoms could be considered explicitly, as is done in molecular mechanics programs.<sup>14,21,28</sup> Jackson<sup>33</sup> has interpreted the changes in bond dissociation energies from methane to isobutane in terms of hybridization and van der Waals interactions. Such refinements are not yet necessary for the 23 molecules considered here.

The method could be extended in several ways. Isopropyl derivatives agreed well with the expression of Luo and Benson<sup>17</sup> and should work well with the present model. Indeed, propane and isobutane already appear in Table II. The method could be extended to ethers, thioethers, secondary and tertiary amines,

larger alkyl groups, and other substituents, X. It could be extended to di-, tri-, and polysubstituted alkanes if induced dipoles or van der Waals forces are included.<sup>11,15</sup> Following Benson and Luria<sup>4</sup> it could be extended to radicals and alkenes. Once it has been refined, it could be made accessible in molecular mechanics programs, where it might reduce the number of input parameters required or provide better understanding of the forces involved. With the inclusion of appropriate induced dipoles, it could be used to calculate molecular dipole moments and intermolecular forces.

As it stands, the method does provide a simple, quantitative explanation for the interesting effects of methyl groups on molecular stability in Table II; an explanation which has been lacking for more than 20 years.<sup>1</sup>

**Acknowledgment.** The authors wish to thank Y.-R. Luo, T. S. Cameron, D. R. Arnold, T. B. Grindley, J. Wang, N. Cann, K. V. Darvesh, M. A. White, and P. G. Kusalik for valuable discussions and the Natural Sciences and Engineering Research Council of Canada for financial support.

(33) Jackson, R. A. *Tetrahedron* 1991, 47, 6777-6786.

## Computer Simulation of the CO<sub>2</sub>/HCO<sub>3</sub><sup>-</sup> Interconversion Step in Human Carbonic Anhydrase I

Johan Åqvist,\*<sup>†</sup> Michael Fothergill,<sup>†</sup> and Arieh Warshel\*<sup>‡</sup>

*Contribution from the Department of Molecular Biology, Uppsala University, Uppsala Biomedical Centre, Box 590, S-75124 Uppsala, Sweden, and Department of Chemistry, University of Southern California, Los Angeles, California 90089-1062.  
Received February 17, 1992*

**Abstract:** The CO<sub>2</sub>/HCO<sub>3</sub><sup>-</sup> interconversion step in human carbonic anhydrase I is simulated using the empirical valence bond (EVB) method in combination with free energy perturbation molecular dynamics calculations. The calculated free energy profile for the enzyme reaction is found to be in reasonable agreement with experimental kinetic data. The simulations show that the enzyme is able to reduce both the activation barrier as well as the exothermicity of the interconversion step (compared to the water reaction). The catalytic zinc ion appears to be important for both of these effects, its strong interaction with the reacting hydroxide ion being a key element of the catalytic effect. The predicted conformation of the HCO<sub>3</sub><sup>-</sup> complex with the enzyme is similar to that observed experimentally for a mutant version of isozyme II. The geometry of the transition state generated by the EVB simulations is compared to ab initio studies of model systems and also to some relevant experimental inhibitor complexes. The simulated energetics of the uncatalyzed solution reaction is used to estimate the reaction free energy in vacuo, and the results are found to be in good agreement with high-level basis set ab initio calculations.

### Introduction

One of the most interesting challenges facing computational chemistry today is to be able to model catalytic reactions in enzymes in a quantitative way. The prospects for this type of "computational enzymology" approach to be successful are beginning to look rather promising, owing to both theoretical advances as well as increased computer power.<sup>1,2</sup> In this paper we report simulations of the CO<sub>2</sub>/HCO<sub>3</sub><sup>-</sup> interconversion step in human carbonic anhydrase I (HCAI). The empirical valence bond (EVB) method<sup>1</sup> is used for constructing the reaction potential energy surface, and the free energy perturbation (FEP) technique combined with molecular dynamics (MD) simulation is employed to evaluate reaction free energy profiles. The results from the simulations are found to be in reasonable agreement with experimental estimates of the reaction energetics,<sup>3f,g</sup> and they emphasize the important multiple functions of the active site metal during the catalytic process.

Carbonic anhydrase (CA) is an example of a metalloenzyme that serves as a useful test case for theoretical studies of the role of metal ions in enzyme catalysis, since it has been subjected to

extensive experimental investigations, both with respect to structure and function.<sup>3</sup>

(1) Warshel, A. *Computer Modeling of Chemical Reactions in Enzymes and in Solutions*; Wiley: New York, 1991.

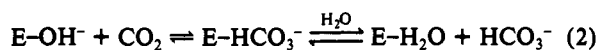
(2) (a) Warshel, A.; Levitt, M. *J. Mol. Biol.* 1976, 103, 227. (b) van Duijnen, P. Th.; Thole, B. Th.; Hol, W. G. J. *Biophys. Chem.* 1979, 9, 273. (c) Tapia, O.; Johannin, G. *J. Chem. Phys.* 1981, 75, 3624. (d) Warshel, A. *Proc. Natl. Acad. Sci. U.S.A.* 1984, 81, 44. (e) Weiner, S. J.; Seibel, G. L.; Kollman, P. A. *Proc. Natl. Acad. Sci. U.S.A.* 1986, 83, 649. (f) Rao, S. N.; Singh, U. C.; Bash, P. A.; Kollman, P. A. *Nature* 1987, 328, 551. (g) Warshel, A.; Sussman, F.; Hwang, J.-K. *J. Mol. Biol.* 1988, 201, 139. (h) Singh, U. C. *Proc. Natl. Acad. Sci. U.S.A.* 1988, 85, 4280. (i) Åqvist, J.; Warshel, A. *Biochemistry* 1989, 28, 4680. (j) Åqvist, J.; Warshel, A. *J. Am. Chem. Soc.* 1990, 112, 2860. (k) Bash, P. A.; Field, M. J.; Davenport, R. C.; Petsko, G. A.; Ringe, D.; Karplus, M. *Biochemistry* 1991, 30, 5826. (l) Waszkowycz, B.; Hillier, I. H.; Gensmantel, N.; Payling, D. W. *J. Chem. Soc., Perkin Trans. 2* 1991, 225.

(3) (a) Liljas, A.; Kannan, K. K.; Bergstén, P.-C.; Waara, I.; Fridborg, K.; Strandberg, B.; Carlbom, U.; Järup, L.; Lövgren, S.; Petef, M. *Nature New Biol.* 1972, 235, 131. (b) Kannan, K. K.; Ramanadham, M.; Jones, T. A. *Ann. N.Y. Acad. Sci.* 1984, 429, 49. (c) Eriksson, A. E.; Kylsten, P. M.; Jones, T. A.; Liljas, A. *Proteins* 1988, 4, 283. (d) Lindskog, S.; Engberg, P.; Forsman, C.; Ibrahim, S. A.; Jonsson, B.-H.; Simonsson, I.; Tibell, L. *Ann. N.Y. Acad. Sci.* 1984, 429, 61. (e) Silverman, D. N.; Lindskog, S. *Acc. Chem. Res.* 1988, 21, 30. (f) Behravan, G. *Studies of Site-Specific Mutants of Carbonic Anhydrase*. Ph.D. Thesis, University of Umeå, 1990. (g) Behravan, G.; Jonsson, B.-H.; Lindskog, S. *Eur. J. Biochem.* 1990, 190, 351.

<sup>†</sup>Uppsala University.

<sup>‡</sup>University of Southern California.

The reaction catalyzed by CA, viz., the reversible hydration of carbon dioxide, can be described as<sup>3c</sup>



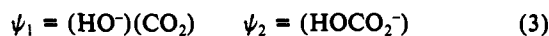
Here, eq 1 represents the proteolysis of the reacting active-site water molecule and subsequent transfer of a proton from the active site to the surrounding solution, while eq 2 denotes the "half-reaction" corresponding to the interconversion between  $\text{CO}_2$  and  $\text{HCO}_3^-$ . The former half-reaction has been found to be rate limiting both in isozymes I and II,<sup>3e,f</sup> although it is not known exactly where on the proton-transfer pathway (eq 1) the rate-limiting barrier is located.

Various earlier theoretical studies have examined the  $\text{CO}_2/\text{HCO}_3^-$  interconversion process with ab initio and semiempirical MO methods for model systems in vacuo.<sup>4,5,18</sup> Solvation effects on an ab initio energy profile have also recently been reported for the uncatalyzed reaction.<sup>5</sup> Merz has evaluated the energetics of  $\text{CO}_2$  binding and the  $\text{pK}_a$  of Glu106 in HCAII by FEP methods,<sup>6</sup> and Liang and Lipscomb have also studied  $\text{CO}_2$  binding and diffusion inside the enzyme with MD simulations.<sup>7</sup>

We have recently carried out simulations of the initial proton-transfer step (the first part of eq 1) in HCAI using the EVB/FEP/MD approach.<sup>8</sup> This study yielded a proton-transfer rate very close to the observed overall rate of the enzyme, although it is not clear whether it actually is the initial water ionization that represents the highest barrier on the proton translocation pathway. Furthermore, the  $\text{pK}_a$  associated with the ionization of the zinc-bound water molecule was evaluated and found to be about 7.4, which also appears to be in the range observed experimentally.<sup>3f,9</sup> Here, we will now focus on the first part of eq 2, viz., the subsequent  $\text{CO}_2/\text{HCO}_3^-$  interconversion step.

## Methods

We describe the interconversion reaction by the two VB structures



The energies of these two states are written as

$$\epsilon_i = H_{ii} = \sum_j \Delta M_j^{(i)}(b_j^{(i)}) + \frac{1}{2} \sum_m \gamma_m^{(i)} k_m^{(i)} (\theta_m^{(i)} - \theta_{0,m}^{(i)})^2 + \sum_r K_r^{(i)} [1 + \cos(n_r^{(i)} \phi_r^{(i)} - \delta_r^{(i)})] + V_{\text{nb},rr}^{(i)} + \alpha^{(i)} + V_{\text{nb},rs}^{(i)} + V_s \quad (4)$$

where  $\Delta M_j^{(i)}$  denotes the Morse potential corresponding to the  $j$ th bond in the  $i$ th VB structure, and the second term and third terms, respectively, denote the bond angle and torsional angle bending contribution. The fourth term denotes the nonbonded interactions between the reacting groups (subscript  $r$ ). The nonbonded interaction with the surrounding protein and solvent ( $s$ ) is denoted by  $V_{\text{nb},rs}^{(i)}$ , and the parameters  $\alpha^{(i)}$  in eq 4 will enter as the difference ( $\Delta\alpha = \alpha^{(2)} - \alpha^{(1)}$ ) in energy between  $\psi_2$  and  $\psi_1$  with the reacting fragments at infinite separation in the gas phase and are obtained as described earlier<sup>2a,i</sup> from solution experiments.<sup>10</sup> The last term represents the internal potential energy

of the surrounding protein/solvent medium. The EVB ground-state surface  $E_g$  is obtained from  $\text{HC}_g = E_g \text{C}_g$ , where the diagonal elements of  $\text{H}$  are given by eq 4. The off-diagonal matrix elements are approximated by a simple exponential function,<sup>28</sup>  $H_{12} = A_{12} e^{-r_{12}/r_{\text{OC}}}$ , where  $r_{\text{OC}}$  denotes the separation between the atoms forming the new bond. The free energy function corresponding to the ground-state potential,  $E_g$ , is calculated using a combination of FEP and umbrella sampling as described in earlier work<sup>28,i,8</sup>

$$\exp\{-\Delta g(X^n)/RT\} \approx \exp\{-\Delta G(\bar{\lambda}_m)/RT\} \langle \exp\{-[E_g(X^n) - \epsilon_m(X^n)]/RT\} \rangle_m \quad (5)$$

where  $\Delta G(\bar{\lambda}_m)$  is the free energy on the effective perturbation potential and the reaction coordinate,  $X^n$ , is defined in terms of the energy gap,  $\Delta\epsilon = \epsilon_1 - \epsilon_2$ , between the two states of eq 4.<sup>1</sup> The experimental data on  $\text{CO}_2$  hydration in aqueous solution from ref 10 was used to calibrate the  $\Delta\alpha$  and  $H_{12}$  parameters of the EVB Hamiltonian by simulating the reaction in a surface restrained droplet<sup>11</sup> of water containing 200 solvent molecules (see below). As in our earlier simulations of the initial PT step, the GROMOS "extended atom" potential<sup>12a</sup> was used in order to reduce the computational cost. The calculations were carried out with a version of the MOLARIS program<sup>12b</sup> modified to incorporate this potential.<sup>12c</sup> The oxygen Lennard-Jones parameters for charged carboxylate groups (in our case Glu106, Glu117, and  $\text{HCO}_3^-$ ) were determined by calculating the free energy of hydration for the acetate ion while retaining the standard GROMOS charge distribution for the carboxylate moiety. The resulting parameters ( $A_O = 956.0$ ,  $B_O = 23.0$ ) yield a free energy for charging the ion of  $-79.0 \pm 0.4$  kcal/mol (the free energy of creating the uncharged atoms in water is expected to be about 2.0 kcal/mol)<sup>13</sup> in agreement with experimental estimates for the hydration energy of acetate.<sup>14</sup> All other parameters and details of the simulations (time-step, cutoff radii, etc.) were identical with those used in ref 6 except that the trajectories in this case consisted of 15 ps of equilibration and 70 ps of data sampling. In this context, a comment on the convergence of free energy simulations might be in place since some recent studies<sup>22</sup> have given the impression that simulation lengths of several hundred picoseconds are required to obtain reasonable accuracy. These studies, however, deal with processes such as hydrophobic hydration which are dominated by weak and short-ranged forces (van der Waals and dipole-dipole interactions), and adequate phase-space sampling will therefore take longer time (the relative magnitude of errors will also be rather large since the calculated quantities are always small). On the other hand, for systems in which strong and long-ranged electrostatic forces dominate, it seems that these convergence problems are not at all as severe.<sup>12c,23,24</sup> For such systems, however, the treatment of long-range forces as well as boundary conditions are extremely important and neither truncation by cutoff radii nor periodic boundary conditions are in this case particularly good solutions.<sup>11,12c,23</sup>

## Results and Discussion

The forward and reverse rates for the uncatalyzed attack of  $\text{OH}^-$  on  $\text{CO}_2$  in water are given in ref 10a (see also ref 10b) as  $1.1 \times 10^4 \text{ s}^{-1}$  and  $1.9 \times 10^{-4} \text{ s}^{-1}$ , respectively. Using the transition-state theory approximation with a transmission factor of unity, one thus obtains values of  $\Delta G^\ddagger = -10.5$  kcal/mol and  $\Delta G^\ddagger = +11.9$  kcal/mol for the reaction and activation free energies.

(4) (a) Jönsson, B.; Karlström, G.; Wennerström, H. *J. Am. Chem. Soc.* **1978**, *100*, 1658. (b) Pullman, A. *Ann. N.Y. Acad. Sci.* **1981**, *367*, 340. (c) Cook, C. M.; Allen, L. C. *Ann. N.Y. Acad. Sci.* **1984**, *429*, 84. (d) Liang, J.-Y.; Lipscomb, W. N. *J. Am. Chem. Soc.* **1986**, *108*, 5051. (e) Liang, J.-Y.; Lipscomb, W. N. *Biochemistry* **1988**, *27*, 8676. (f) Merz, K. M., Jr.; Hoffmann, R.; Dewar, M. J. S. *J. Am. Chem. Soc.* **1989**, *111*, 5636. (g) Jacob, O.; Cardenas, R.; Tapia, O. *J. Am. Chem. Soc.* **1990**, *112*, 8692. (5) Peng, Z.; Merz, K. M., Jr. *J. Am. Chem. Soc.* **1992**, *114*, 2733. (6) (a) Merz, K. M., Jr. *J. Am. Chem. Soc.* **1991**, *113*, 406. (b) Merz, K. M., Jr. *J. Am. Chem. Soc.* **1991**, *113*, 3572. (7) Liang, J.-Y.; Lipscomb, W. N. *Proc. Natl. Acad. Sci. U.S.A.* **1990**, *87*, 3675. (8) Åqvist, J.; Warshel, A. *J. Mol. Biol.* **1992**, *224*, 7. (9) Campbell, I. D.; Lindskog, S.; White, A. I. *J. Mol. Biol.* **1974**, *90*, 469.

(10) (a) Magid, E.; Turbeck, B. O. *Biochim. Biophys. Acta* **1968**, *165*, 515. (b) Pinsent, B. R. W.; Pearson, L.; Roughton, F. J. W. *Trans. Faraday Soc.* **1956**, *52*, 1512.

(11) King, G.; Warshel, A. *J. Chem. Phys.* **1989**, *91*, 3647.

(12) (a) van Gunsteren, W. F.; Berendsen, H. J. C. *Groningen Molecular Simulation (GROMOS) Library Manual*; Biomos B. V., Nijenborgh 16, Groningen, The Netherlands, 1987. (b) Warshel, A.; Creighton, S. In *Computer Simulation of Biomolecular Systems*, van Gunsteren, W. F., Weiner, P. K., Eds.; ESCOM: Leiden, 1989; p 120. (c) Åqvist, J. *J. Phys. Chem.* **1990**, *24*, 8021.

(13) Ben-Naim, A.; Marcus, Y. *J. Chem. Phys.* **1984**, *81*, 2016.

(14) See, e.g., the compilation in: Cramer, C. J.; Truhlar, D. G. *J. Am. Chem. Soc.* **1991**, *113*, 8305.

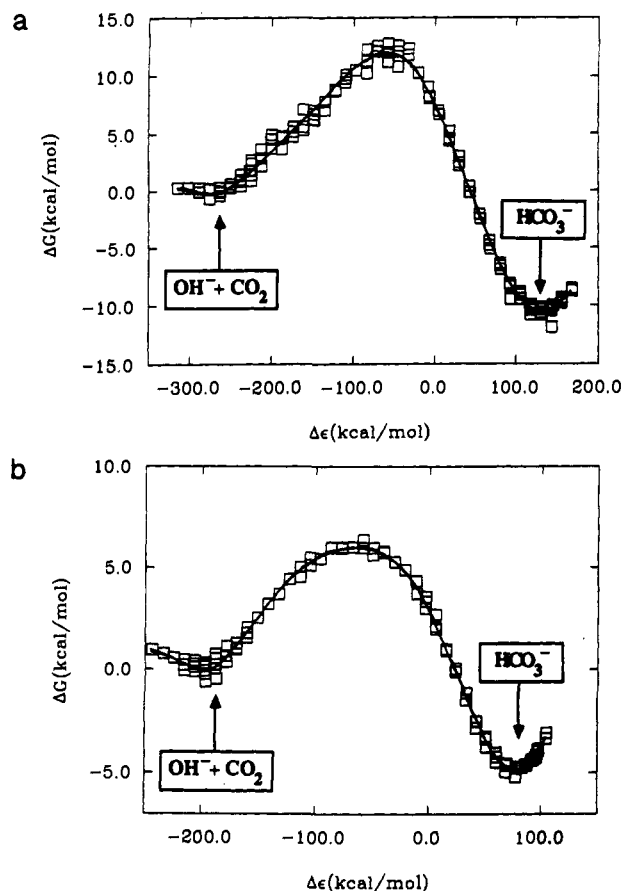
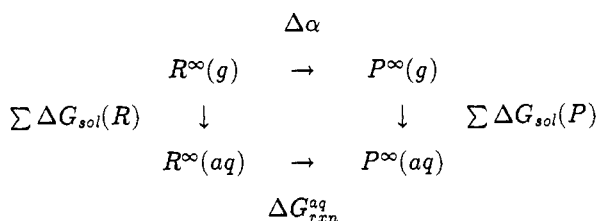


**Figure 1.** (a) Calculated free energy profile for the reference reaction in water after calibration of the  $\Delta\alpha$  and  $H_{12}$  parameters. The reaction coordinate  $\Delta\epsilon$  denotes the energy gap between the two diabatic surfaces.<sup>28</sup> (b) Calculated free energy profile for the interconversion reaction (eq 2) in the active site of HCAI.

Figure 1a shows the calculated free energy profile for the *solution* reaction after calibrating the EVB Hamiltonian with respect to the  $\Delta\alpha$  and  $H_{12}$  parameters ( $\Delta\alpha = -15.8$  kcal/mol,  $A_{12} = 107.5$  kcal/mol,  $\mu_{12} = 0.40$  Å<sup>-1</sup>). One can note in the case where  $|H_{12}| \rightarrow 0$  as  $|\Delta\epsilon| \rightarrow \infty$ ,  $\Delta\alpha$  is determined by the thermodynamic cycle



where  $R^\infty$  and  $P^\infty$  denote the reactant and product states with the relevant fragments noninteracting. The way we have defined the  $H_{12}$  function above, however, will add an extra (constant) term to the energy at the product. This term can be evaluated from a series expansion of the ground-state energy (provided that  $2H_{12}/|\epsilon_1 - \epsilon_2| < 1$ ) which yields

$$E_g = \min(\epsilon_1, \epsilon_2) - \frac{H_{12}^2}{|\epsilon_1 - \epsilon_2|} + \frac{H_{12}^4}{|\epsilon_1 - \epsilon_2|^3} - \dots \quad (6)$$

Inserting the average simulation values of  $H_{12}$  and  $\Delta\epsilon$  at the product (61.9 and 141.3 kcal/mol, respectively) gives the extra contribution  $\Delta E_{\text{offd}} = -23.3$  kcal/mol that should be added to the gas-phase shift,  $\Delta\alpha$ , in order to be consistent with the thermodynamic cycle above ( $\Delta\alpha_{\text{eff}} = \Delta\alpha + \Delta E_{\text{offd}} = -39.1$  kcal/mol). It is thus possible to get a back-of-the-envelope check of the consistency of the computational reaction model from<sup>1</sup>

$$\Delta G_{rxn}^{aq} - \Delta\alpha_{\text{eff}} = \Delta\Delta G_{sol}^{R \rightarrow P} \quad (7)$$

Insertion of the relevant numbers yields  $\Delta\Delta G_{sol}^{R \rightarrow P} = +30.4$  kcal/mol which is in good agreement experimental estimates for the difference in solvation free energies.<sup>15</sup> Thus, this type of check shows that the model for the solution reaction is physically consistent with experimental data.

It is also interesting to note that, in vacuo, the interconversion reaction is barrierless and exothermic by 47–49 kcal/mol<sup>4d,5</sup> (it seems that most of the gas-phase quantum mechanical calculations have not reproduced this energy profile quantitatively, the exception being the recent high-level basis set (MP4/6-311++-G\*\*) computations by Peng and Merz<sup>5</sup>). The difference in solvation energy between OH<sup>-</sup> and HCO<sub>3</sub><sup>-</sup> and the delocalization of charge along the reaction pathway, with which is associated a solvent reorganization barrier, thus produces a reaction profile in solution that is very different from the gas phase. As is evident from eq 7, the quantity  $\Delta\alpha$  is the gas-phase free energy which can be obtained from heats of formation, e.g., if the  $\Delta S$  contribution can be estimated. The value of  $\Delta\alpha_{\text{eff}} = -39.1$  kcal/mol obtained in our case can be compared to the experimental estimate of -38.2 kcal/mol given in ref 5. Hence, we could just as well have calibrated the EVB Hamiltonian against *gas-phase* experimental data and would still have obtained a very accurate value for  $\Delta G_{rxn}$  in water.

After calibrating the EVB surface for the solution reaction, we can now turn to the calculation of the same reaction catalyzed by HCAI, without any reparametrization of the EVB Hamiltonian. The resulting free energy profile for the enzyme catalyzed reaction is shown in Figure 1b. Two important features of the enzyme profile can be immediately appreciated from the figure. Firstly, the activation barrier for the nucleophilic attack is reduced by the enzyme (by 5–6 kcal/mol), and, secondly, the relative stability of the states  $\psi_1$  and  $\psi_2$  is shifted such that this reaction step becomes less exothermic than in water. The calculated values for  $\Delta G^\ddagger$  and  $\Delta G^\circ$  are 6.3 kcal/mol and -4.8 kcal/mol, respectively, with convergence errors of  $\pm 1.6$  kcal/mol. Here, it should be noted that the lowering of the transition state for the interconversion process is much less than for the preceding water ionization step.<sup>8</sup> That is, the rate enhancement (compared to water) of the PT step was calculated to be about a factor of 10<sup>8</sup> while the rate acceleration for the OH<sup>-</sup> attack on CO<sub>2</sub> is only about 10<sup>3</sup>–10<sup>4</sup>. The latter reaction is, however, already quite rapid in solution,<sup>10</sup> and the enzyme does probably not need to put a larger effort into reducing the interconversion barrier since a reduction of a few kcal/mol is enough to not make it rate-limiting overall.<sup>8</sup>

The simulations also show that the "reactants" ( $\psi_1$ ) are in this case stabilized relative to the product ( $\psi_2$ ). This reflects the strong interaction between the zinc and OH<sup>-</sup> ions that is also essential for making the OH<sup>-</sup> nucleophile available at a low energetic cost. Moreover, it is important from the functional viewpoint that the enzyme is able to "level out" the free energy difference between  $\psi_1$  and  $\psi_2$  somewhat since there are requirements for it to operate also in the reverse direction. The calculated free energy profile for the CO<sub>2</sub>/HCO<sub>3</sub><sup>-</sup> interconversion step appears to be in reasonable agreement with the experimental data of Behravan et al.<sup>38</sup> These authors have estimated the forward and reverse rate constants for the nucleophilic attack in HCAI as  $3.4 \times 10^7$  s<sup>-1</sup> and  $3.8 \times 10^4$  s<sup>-1</sup>, respectively, yielding values of  $\Delta G^\circ = -4.1$  kcal/mol and  $\Delta G^\ddagger = 7.1$  kcal/mol. The average conformation of the reactant state in our simulations has the CO<sub>2</sub> molecule in a similar position to those found by Liang and Lipscomb<sup>7</sup> and by Merz.<sup>6a</sup> However, the binding site that was named A in ref 6a appears to be located slightly further into the hydrophobic pocket compared to our initial conformation (which, on the other hand, also seems to be an energy minimum with respect to CO<sub>2</sub> binding). It may therefore be that a small amount of energy (~1–2 kcal/mol) is required in order to bring carbon dioxide from its most favorable "binding site" into a reactive position, but this issue has not been addressed in our simulations.

(15) The experimental estimate for this quantity is about 29–31 kcal/mol. See refs 14 and 5 and: Warshel, A.; Russell, S. T. *Q. Rev. Biophys.* 1984, 17, 283.

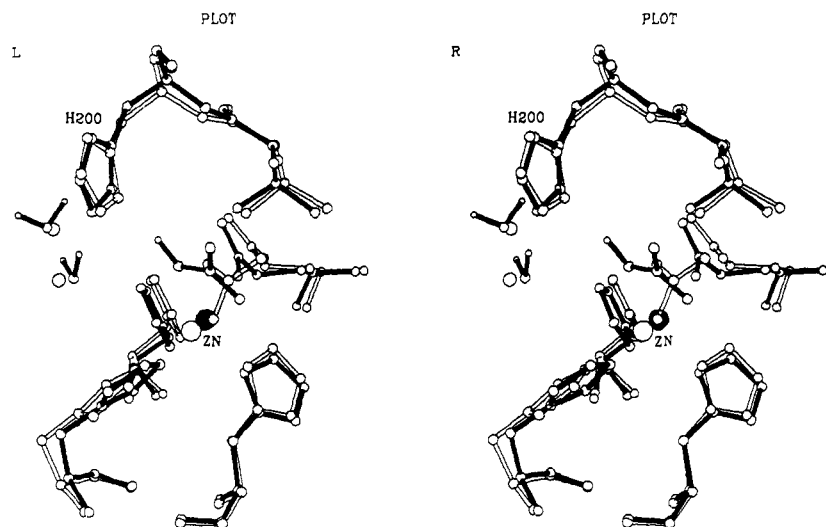


**Figure 2.** Comparison of the average MD structure of the HCAI-bicarbonate complex with that of the same complex in the T200H mutant of HCAII.<sup>17</sup> The simulated structure is depicted with black bonds and the  $Zn^{2+}$  ion is in this case also drawn in black.

Just as for the water ionization step, it seems clear that the zinc ion plays a major role also in controlling the energetics of the interconversion step. One reason for the stabilization of  $\psi_1$  and the subsequent transition state relative to the product is clearly the stronger interaction between  $Zn^{2+}$  and  $OH^-$  than the corresponding one with  $HCO_3^-$ . Moreover, when the product is formed it will inevitably find some of its negative charge located in a relatively hydrophobic environment, although the region is not completely devoid of dipolar groups (in particular, the backbone-NH group of Thr199 interacts with the carboxylate moiety of the product). It thus appears that the active site microenvironment is well suited to actually *destabilize* the product (compared to the solution reaction) somewhat, thereby enabling the reversibility of the interconversion process. Furthermore, it should be noted that the so-called reorganization energy (see, e.g., refs 1 and 16) both at reactants and products is reduced by the enzyme compared to the solution reaction. This indicates that the change in polarization of the active site, in response to the changing charge distribution during the reaction, is smaller than the corresponding one in water (this type of effect has also been observed earlier<sup>16</sup>). Here again, the zinc ion is likely to be important together with other polar groups of the active site. Xue et al.<sup>17</sup> have recently determined the crystal structure of the Thr200  $\rightarrow$  His mutant of HCAII in complex with the substrate/product  $HCO_3^-$ . This mutant thus mimicks the structure of HCAI which has a histidine residue in position 200. It has also been found that the catalytic parameters of the T200H mutant have changed in the direction of HCAI.<sup>38</sup> In particular, the affinity of T200H and of HCAI for bicarbonate is about 1.5–1.8 kcal/mol more favorable than for native HCAII.<sup>38</sup> Figure 2 shows a comparison between the crystal structure of Xue et al.<sup>17</sup> and a 4-ps average MD structure at the product state ( $\psi_2$ ) with  $HCO_3^-$  bound. It can be seen that the position of the bicarbonate molecule is rather similar in the two cases, the main difference being a slight rotation about the C–OH bond (this rotation determines whether the  $HCO_3^-$  hydrogen is pointing toward this 200 ND1 or Thr 199 OG1, both of which seem to provide good hydrogen bond acceptors). Furthermore, in both cases the hydroxyl group is still ligated to the  $Zn^{2+}$  ion, and no rotation of the bicarbonate molecule, which would bring the two carboxylate oxygens into the metal coordination sphere, has occurred. Interactions with the peptide –NH group of Thr199 and the side chain of His200 are evident, and the latter of these could possibly explain the increased affinity for  $HCO_3^-$

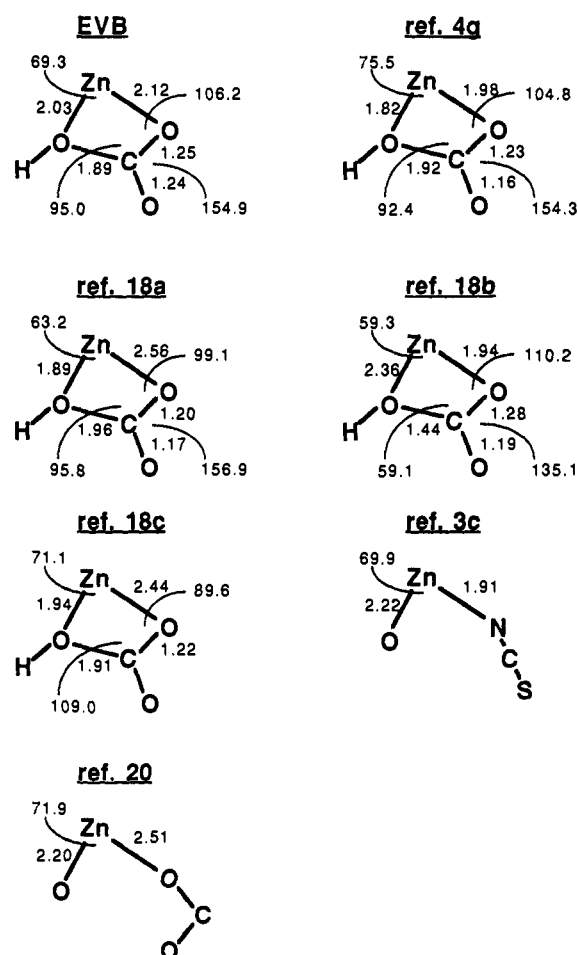


**Figure 3.** Comparison of the average transition-state geometry from the EVB simulations with those from the ab initio SCF calculations of Tapia et al.,<sup>4g,18a</sup> Solà et al.,<sup>18b</sup> and Krauss and Garmer.<sup>18c</sup> Three ammonia molecules were used to model the  $Zn^{2+}$  ligands in ref 18. The figure also shows the observed coordination geometries of the inhibitors  $SCN^-$  and  $HCOO^-$  bound to HCAII.<sup>3c,20</sup>

that is observed when the amino acid in position 200 is a histidine.<sup>38</sup> Note also the excellent agreement between calculated and observed positions for the two water molecules near His200.

Another point which is interesting in the context of methodology is the comparison of the transition state (TS) structure in the enzyme obtained by the EVB method to the corresponding ones

(16) (a) Yadav, A.; Jackson, R. M.; Holbrook, J. J.; Warshel, A. *J. Am. Chem. Soc.* **1991**, *113*, 4800. (b) Warshel, A.; Hwang, J. K.; Aqvist, J. *Faraday Discuss.* **1992**, *93*, 000.

(17) Xue, Y.; Vidgren, J.; Svensson, L. A.; Liljas, A.; Jonsson, B.-H.; Lindskog, S. In preparation.

from gas-phase ab initio calculations. Tapia and co-workers have located the saddle point for the interconversion step in vacuo in the presence of bare<sup>48</sup> as well as ammonia-ligated Zn<sup>2+</sup>.<sup>18a</sup> Optimized TS structures with NH<sub>3</sub>-ligated zinc have also been obtained recently using different basis sets by Solà et al.<sup>18b</sup> and by Krauss and Garmer.<sup>18c</sup> These four ab initio structures are shown in Figure 3 together with the time-averaged EVB TS structure. Here, a note of caution should perhaps be given concerning the ammonia-ligated ab initio structures. If the product state (HCO<sub>3</sub><sup>-</sup>) is artificially stabilized by the interaction with an ammonia molecule such as in ref 18c, this will make the TS look "earlier", i.e., shorter Zn-OH distance and longer Zn-CO<sub>2</sub> distance, than would be the case without such an interaction (the imidazole ligands in CA do not have the same capability of hydrogen-bonding to the substrate). Although the TS geometries for these relatively simple vacuum systems clearly depend on basis sets and the model used for the metal ligands, the comparison in Figure 3 suggests at least that the general features of the TS sampled in the EVB simulations are similar to those obtained from ab initio studies on model systems. The differences mainly pertain to the degree of tetra- versus pentacoordination, and in this respect our model for Zn<sup>2+</sup> could probably also be refined, e.g., by including angular terms. However, the energetics calculated here is not likely to be much affected, in particular since the catalytic effect is largely of electrostatic nature and therefore not so sensitive to small changes in geometry. It is, however, essential that the strength of the Zn<sup>2+</sup>-OH<sup>-</sup> interaction is correctly modelled, and in our case this has been verified by calculations of the pK<sub>a</sub> of the corresponding aquo cation.<sup>19</sup> In principle, one would, of course, also want to verify this for the Zn<sup>2+</sup>-HCO<sub>3</sub><sup>-</sup> interaction. In any case, the fact that our HCAI calculations agree with the experimental energetics of the enzyme indicates that the latter interaction is reasonably well modelled.

Also shown in Figure 3 are the coordination geometries of two experimentally determined inhibitor structures of HCAII, namely, the complexes with SCN<sup>-</sup> and HCOO<sup>-</sup>.<sup>3c,20</sup> It is, of course, difficult to say to what extent these inhibitors mimic the actual TS of the interconversion reaction in the enzyme, but their structures seem to be compatible with the overall picture emerging from the theoretical results of Figure 3.

(18) (a) Tapia, O.; Jacob, O.; Colonna, F. *Theor. Chim. Acta* **1992**, in press. (b) Solà, M.; Lledós, A.; Duran, M.; Bertrán, J. *J. Am. Chem. Soc.* **1992**, *114*, 869. (c) Krauss, M.; Garmer, D. R. *J. Am. Chem. Soc.* **1991**, *113*, 6426.

(19) Åqvist, J. *J. Mol. Struct. (THEOCHEM)* **1992**, *256*, 135.

(20) Håkansson, K.; Carlsson, M.; Svensson, L. A.; Liljas, A. In preparation.

### Concluding Remarks

The present work has used an EVB/FEP/MD computer simulation approach to model the CO<sub>2</sub>/HCO<sub>3</sub><sup>-</sup> interconversion reaction in HCAI and to correlate the structure of the enzyme active site with its catalytic function. The agreement as far as energetics is concerned between the calculations and the experimental kinetic data of Lindskog and co-workers<sup>8</sup> is remarkably good considering the fact that no part of the force field has been specifically tailored for carbonic anhydrase (in particular not the zinc model). Both the present work as well as our previous study of the initial proton-transfer step in HCAI indicate that the Zn<sup>2+</sup> ion contributes in a major way to the catalytic effect of the enzyme. This is, of course, not so surprising and the electrostatic stabilization effect was indeed recognized quite early.<sup>21</sup> However, what was less clear was the actual magnitude of the contribution from the Zn<sup>2+</sup> ion, and it has been particularly hard to assess the direct effect of the ion in the interconversion step. Our results suggest that the stabilization of the hydroxide ion by the metal is the most important element of the catalytic effect, since it translates into "multiple" functions for the Zn<sup>2+</sup> ion. That is, this interaction gives a *stabilization* of the "product" in the first (PT) step of the reaction and a *destabilization* of the product in the subsequent interconversion step. It is also likely that the destabilization of bicarbonate, which is necessary in order for the reaction to be reversible, is facilitated by the hydrophobic pocket of the active site in which the product will have to accommodate some of its negative charge. One should note that any energetic questions of the type above which are intimately related to the dielectric properties of the enzyme active site, are almost impossible to address (at least quantitatively) without knowledge of the effective dielectric constant associated with the specific interactions involved. Thus, the value of microscopic simulations, such as the one presented here, is in allowing one to estimate quantitatively the effect of the catalytic ion and the surrounding microenvironment.

**Acknowledgment.** This work was supported by grants from the Swedish National Science Research Council (NFR) and the National Institutes of Health (Grant GM24492). M.F. is the recipient of a postdoctoral fellowship from the foundation Wenner-Grenska Samfundet.

(21) (a) Werber, M. M. *J. Theor. Biol.* **1976**, *60*, 51. (b) Woolley, P. *Nature* **1975**, *258*, 677.

(22) (a) Pearlman, D. A.; Kollman, P. A. *J. Chem. Phys.* **1991**, *94*, 4532. (b) Straatsma, T. P.; McCammon, J. A. *J. Chem. Phys.* **1991**, *95*, 1175. (c) Mitchell, M. J.; McCammon, J. A. *J. Comput. Chem.* **1991**, *12*, 271.

(23) Lee, F. S.; Warshel, A. *J. Chem. Phys.* **1992**, *97*, 3100.

(24) (a) Straatsma, T. P.; Berendsen, H. J. C. *J. Chem. Phys.* **1988**, *89*, 5876. (b) Mazar, M. H.; McCammon, J. A.; Lybrand, T. P. *J. Am. Chem. Soc.* **1989**, *111*, 56.